A theoretical study of the static structure of the Na_xK_{1-x} liquid alloy

1996 J. Phys.: Condens. Matter 8 4465

(http://iopscience.iop.org/0953-8984/8/25/005)

J. Phys.: Condens. Matter **8** (1996) 4465–4483. Printed in the UK

A theoretical study of the static structure of the Na_xK_{1-x} liquid alloy

L E González†, D J González†, A Meyer‡ and M Silbert§

† Departamento de Física Teórica, Facultad de Ciencias, Universidad de Valladolid, 47011 Valladolid, Spain‖

‡ Department of Physics, Northern Illinois University, DeKalb, IL 60115, USA

§ School of Physics, University of East Anglia, Norwich NR4 7TJ, UK

Received 3 January 1996, in final form 11 April 1996

Abstract. We present theoretical calculations for the static structure and ordering properties of the Na–K liquid alloy. Our theoretical approach is based on the neutral pseudoatom method for deriving the interatomic pair potentials, and on the modified-hypernetted-chain theory of liquids for obtaining the liquid structure, leading to a whole combination that is free of adjustable parameters. The results obtained predict a weak phase-separating tendency, in good agreement with the available experimental data.

1. Introduction

During the last few years, remarkable progress has been achieved in the theoretical description of the static, thermodynamic, and dynamic properties of simple (*s–p bonded*) liquid metals [1, 2]. This has been mainly due to the combination of pseudopotential perturbation theory with modern accurate liquid-state theories and/or classical computer simulation techniques. The use of accurate pseudopotentials, derived from first principles, combined with the fact that covalent effects are basically negligible in simple liquid metals, has allowed the use of the homogeneous electron gas as the reference state for the perturbative calculation of the energy of the system.

However, when it comes to alloys, the situation is very different. Although much work has been performed in the study of structural and thermodynamic properties of liquid binary alloys by using semiempirical models [1, 3], studies from a more fundamental level are far more scarce. This situation can be explained in terms of one or more of the following reasons. First, the environment of an ion in an alloy can be very different from that of a free atom, where standard pseudopotentials are constructed; therefore, the pseudopotential is likely to change, and transferability problems may arise. Second, the pseudopotential may cease to be weak, and consequently perturbation theory will no longer be valid. Third, covalent/ionic tendencies may appear in the alloy, and the use of the homogeneous electron gas as a reference system will not be appropriate. The second and third problems may be overcome by resorting to first-principles molecular dynamics which uses density functional theory (DFT) instead of perturbation theory, although this approach does usually rely on free-atom computed pseudopotentials.

‖ Fax: 83-423013.

0953-8984/96/254465+19$19.50

In this paper we concentrate on a liquid alloy, namely Na_xK_{1-x}, for which the above second and third problems do not really apply. This system may be considered as a simple liquid alloy where the nearly-free-electron theory holds and, therefore, the pseudopotential perturbation theory can be applied. This fact, combined with the availability of extensive experimental work on this alloy, has motivated an appreciable amount of theoretical work that has already been performed on this system.

In the late sixties, Enderby and North [4] carried out the first theoretical calculation of the x-ray static structure factor at the equiatomic composition. They used the Percus–Yevick (PY) solution for a binary mixture of hard spheres (HS), obtaining results in qualitative agreement with the corresponding experimental results of Henninger *et al* [5]. Moreover, the calculated isothermal compressibility value, derived from the long-wavelength limit of the partial structure factors, showed a good agreement with the experimental results of Abowitz and Gordon [6]. The PY–HS model, combined with a Heine–Abarenkov-type pseudopotential and Ziman's formula, was also used by van der Lugt *et al* [7] to calculate the electrical resistivity of this alloy over the whole concentration range; their results were in good agreement with their own experimental measurements [7], which show a parabolic shape with a maximum located at $x_{Na} \approx 0.5$.

The experimental bulk viscosity, estimated from the ultrasonic measurements of Amaral and Letcher [8], shows a peaked structure at a concentration $0.5 \leqslant x_{Na} \leqslant 0.65$, which has been explained in terms of the existence of concentration fluctuations [9]. A similar peaked structure has also been observed for liquid Na–Cs [10] which is a system with a strong tendency towards homocoordination.

The existence of homocoordination tendencies in the Na_xK_{1-x} liquid alloy at $T = 373$ K, is also predicted from the thermodynamic activity measurements of Cafasso *et al* [11] and Hultgren *et al* [12]. The x-ray and neutron diffraction experiments of van der Lugt *et al* (see [13]), carried out for several concentrations and temperatures, also confirm the tendency towards homocoordination.

Several other theoretical studies, using either semiempirical [14, 15] or more fundamental [16–19] approaches, have also been attempted in an effort to calculate the static structure and/or some thermodynamic magnitudes of this alloy. Those based on semiempirical models have mainly focused on the thermodynamic properties, and although use has been made of fitted concentration-dependent parameters, they have given some insight concerning the interatomic interactions. On the other hand, those studies based on more fundamental approaches have been based on pseudopotential perturbation theory combined with either perturbative or integral equation theories of liquids, and have basically concentrated on the equiatomic composition. For example, Umar *et al* [16] studied the $Na_{0.5}K_{0.5}$ liquid alloy, using the empty-core model (ECM) pseudopotential [20] to derive the interatomic pair potentials in the alloy, and the structure was computed within a perturbative approach using a HS mixture as reference system. A similar scheme, although with a different pseudopotential, was used by Hafner [17] to study the $Na_{0.5}K_{0.5}$ composition. Although both works produced reasonable results for some thermodynamic properties, their static structure results showed no indication of homocoordination tendencies. Similar results were obtained by Singh [18] who used interatomic pair potentials derived from a Heine–Abarenkov-type pseudopotential. Recently, Mori *et al* [19] have studied the static structure of the $Na_{0.5}K_{0.5}$ liquid alloy by combining the Hasegawa *et al* [21] pseudopotential with both molecular dynamics (MD) simulations and the accurate modified-hypernetted-chain (MHNC) theory of liquids. However, although they obtained a very good theory/MD agreement, their structural results gave no indication about homocoordination tendencies.

Therefore, it may be concluded that the main problem is focused on the derivation of

accurate interatomic interactions for this alloy. In this paper we study the static structure of the Na_xK_{1-x} liquid alloy at $T = 373$ K by using effective interatomic pair potentials derived from the neutral-pseudoatom (NPA) method [22–25], whereas the liquid structure is studied by resorting to the MHNC theory of liquids. The ensuing combination results in a calculation that is wholly free of adjustable parameters.

The NPA method has already been successfully applied to the study of the static features of the liquid alkali [26] and alkaline-earth [25] metals. The philosophy of the NPA method is similar to that of the pseudopotential theory, and so is its domain of applicability. In conjunction with DFT, it is entirely *ab initio* and has the advantage of handling true, rather than pseudodensities. In this paper, we first extend the NPA method to simple metallic alloys and we then apply it to the Na_xK_{1-x} liquid alloy.

The MHNC theory used in the evaluation of the liquid structure belongs to the new generation of accurate integral-equation theories of liquids [27]. Its application to various one-component fluids—ranging from simple model potentials to the liquid alkali and alkaline-earth metals—has yielded excellent results for both the structural and thermodynamic properties. Similar conclusions have been obtained for the case of binary mixtures interacting via Lennard-Jones potentials. We briefly discuss the MHNC approximation in section 2.

2. Liquid-state theory

Most of the integral-equation theories of liquids stem from the Ornstein–Zernike equation, which for a homogeneous, isotropic, binary system reads ($i, j = 1, 2$)

$$h_{ij}(r) = c_{ij}(r) + \sum_{l=1}^{2} \rho_l h_{il}(r) * c_{lj}(r) \tag{1}$$

which defines the direct correlation functions, $c_{ij}(r)$, in terms of the total correlation functions $h_{ij}(r) = g_{ij}(r) - 1$, where $g_{ij}(r)$ denote the partial pair distribution functions, and ρ_l denote the partial ionic number densities. Now, equation (1) is supplemented by the exact closure relation

$$c_{ij}(r) = h_{ij}(r) - \ln[g_{ij}(r)\mathrm{e}^{\beta\varphi_{ij}(r)+B_{ij}(r)}] \tag{2}$$

where $\beta = (k_B T)^{-1}$ is the inverse temperature times the Boltzmann constant, the $\varphi_{ij}(r)$ are the interatomic pair potentials, and the $B_{ij}(r)$ denote the so-called bridge functions. In this work we have used the MHNC theory, in which the bridge functions are approximated by those of some reference system. Under this scheme, the actual choice of the bridge functions is mainly determined by the availability of simple expressions for them, either analytic or derived from computer simulation [28–30]. These functions usually depend on some parameters, and different choices of the bridge functions, along with different criteria to determine the parameters, have led to different versions of the MHNC approximation [27, 31, 32]. In practice, a common procedure has been to represent the bridge functions of the system under study by those of a HS system. This approach has led to rather accurate results for the structural and thermodynamic properties of various one-component fluids, ranging from the one-component plasma to Lennard-Jones fluids and simple liquid metals, and also for two-component Lennard-Jones and soft-sphere liquids [31–33].

Other attempts have been made to use the bridge function of a reference system which resembles the system under study more closely than a mixture of additive hard spheres, and on the other hand, to eliminate the need for fixing parameters for the bridge functions. The MHNC-REP approximation, proposed by Levesque *et al* [34] and Mori *et al* [19],

follows this idea, replacing the $B_{ij}(r)$ appearing in equation (2) by those associated with a reference system which is chosen to be the system under study, although interacting with the repulsive part of the interatomic pair potentials; that is

$$\varphi_{ij,rep}(r) = \begin{cases} \varphi_{ij}(r) - \varphi_{ij}(R_{ij}) & r < R_{ij} \\ 0 & r > R_{ij} \end{cases} \tag{3}$$

where the R_{ij} are the positions of the first minimum of the corresponding $\varphi_{ij}(r)$. This choice is based on the assumption that the bridge functions, $B_{ij,rep}(r)$, of this reference system are very similar to the real $B_{ij}(r)$. Now, the $B_{ij,rep}(r)$ are obtained by solving numerically the PY approximation for the $\varphi_{ij,rep}(r)$; this procedure is justified by the empirical observation that the PY approximation is rather accurate for those systems interacting through harshly repulsive short-range forces.

The MHNC-REP approximation has been applied by Mori *et al* to calculate the structural features of the $Na_{0.5}K_{0.5}$ [19], Li_xNa_{1-x} [35] and $Na_{0.5}Cs_{0.5}$ [36] liquid alloys, leading to results in excellent agreement with the corresponding MD simulations.

3. Effective interatomic potentials: the NPA

A simple liquid metallic alloy, A_xB_{1-x}, may be regarded as an assembly of A-type and B-type bare ions with charges Z_v^A and Z_v^B respectively, whose configuration is random in space and time, and embedded in a conduction electron gas of mean density $\bar{n} = \rho[xZ_v^A + (1-x)Z_v^B]$ where ρ is the total ionic number density and x is the concentration of the A-type component. Moreover, the ions attract the valence electrons which pile up around them, thus screening the ionic potentials and leading to effective interactions between the ions.

In this section we briefly describe the method for obtaining the interatomic pair potentials, and for additional details we refer the reader to [22–25].

The present approach for the calculation of the effective interatomic pair potentials involves two distinct steps. First, the valence electronic densities induced by each type of ion when embedded in a homogeneous electron gas with density $\bar{n}$ are obtained by the NPA method; then, in the second step we construct A-type and B-type effective local pseudopotentials which within linear response theory (LRT) reproduce the corresponding induced valence electronic densities as obtained in the first step. Finally, from both pseudopotentials, the effective interatomic pair potentials are obtained. Here, we briefly discuss both steps.

Within the NPA method, it is assumed that the total electronic density, $n_e(\boldsymbol{r})$, of the A_xB_{1-x} alloy, can be decomposed as a sum of single-site, structure-independent and localized electronic densities, $n^{(A)}(r)$ and $n^{(B)}(r)$, which follow the ions in their movement, so (Hartree atomic units will be used through the work)

$$\begin{aligned} n_e(\boldsymbol{r}) &= \sum_i n^{(A)}(|\boldsymbol{r} - \boldsymbol{R}_i^{(A)}|) + \sum_j n^{(B)}(|\boldsymbol{r} - \boldsymbol{R}_j^{(B)}|) \\ &= \sum_i [n_c^{(A)}(|\boldsymbol{r} - \boldsymbol{R}_i^{(A)}|) + n_v^{(A)}(|\boldsymbol{r} - \boldsymbol{R}_i^{(A)}|)] \\ &\quad + \sum_j [n_c^{(B)}(|\boldsymbol{r} - \boldsymbol{R}_j^{(B)}|) + n_v^{(B)}(|\boldsymbol{r} - \boldsymbol{R}_j^{(B)}|)] \end{aligned} \tag{4}$$

where $\boldsymbol{R}_i^{(A)}$ and $\boldsymbol{R}_j^{(B)}$ denote the ionic positions, $n_c^{(A)}(r)$ and $n_c^{(B)}(r)$ are the core electronic densities, and $n_v^{(A)}(r)$ and $n_v^{(B)}(r)$ are the valence electronic densities (screening clouds)

associated with the A-type and B-type ions respectively. The main aim of the NPA method is the computation of $n_v^{(A)}(r)$ and $n_v^{(B)}(r)$; it proceeds as follows.

In a zeroth-order approximation, the alloy can be represented as a homogeneous electron gas of density $\bar{n}$ compensated by a similar positive background of the same density. However, the ions are not distributed uniformly, but are located at positions $\{\boldsymbol{R}_i^{(\alpha)}\}$ ($\alpha = \mathrm{A}, \mathrm{B}$), and create around them a potential $V_{ion}^{(\alpha)}(r)$. Therefore, the previously homogeneous electron density will change by an amount $\Delta n_v(\boldsymbol{r}) = n_v(\boldsymbol{r}) - \bar{n}$, due to the difference between the potential created by the ions and that created by the homogeneous positive background,

$$\Delta V(\boldsymbol{r}) = \sum_i V_{ion}^{(A)}(|\boldsymbol{r} - \boldsymbol{R}_i^{(A)}|) + \sum_j V_{ion}^{(B)}(|\boldsymbol{r} - \boldsymbol{R}_j^{(B)}|) - \left[-\frac{1}{r} * \bar{n}\right] \tag{5}$$

where the symbol * denotes the convolution integral. To compute $\Delta n_v(\boldsymbol{r})$, we rewrite $\Delta V(\boldsymbol{r})$ as

$$\Delta V(\boldsymbol{r}) = \sum_i V_{ion}^{\prime(A)}(|\boldsymbol{r} - \boldsymbol{R}_i^{(A)}|) + \sum_j V_{ion}^{\prime(B)}(|\boldsymbol{r} - \boldsymbol{R}_j^{(B)}|) + V''(\boldsymbol{r}) \tag{6}$$

where

$$V_{ion}^{\prime(A)}(r) = V_{ion}^{(A)}(r) - \left[-\frac{1}{r} * \nu^{(A)}(r)\right] \qquad V_{ion}^{\prime(B)}(r) = V_{ion}^{(B)}(r) - \left[-\frac{1}{r} * \nu^{(B)}(r)\right] \tag{7}$$

and

$$V''(\boldsymbol{r}) = \frac{1}{r} * \left[\bar{n} - \sum_i \nu^{(A)}(|\boldsymbol{r} - \boldsymbol{R}_i^{(A)}|) - \sum_j \nu^{(B)}(|\boldsymbol{r} - \boldsymbol{R}_j^{(B)}|)\right] \equiv \frac{1}{r} * n_r(\boldsymbol{r}) \tag{8}$$

with $\nu^{(A)}(r)$ and $\nu^{(B)}(r)$ being cavity screening functions which integrate to the ionic valences Z_v^A and Z_v^B respectively; they are introduced so as to render $V_{ion}^{\prime(A)}$, $V_{ion}^{\prime(B)}$ and $V''(r)$ as weak as possible. In fact, the choice is mainly determined by requiring that the residual density, $n_r(\boldsymbol{r})$, be small everywhere.

Now, the 'auxiliary ionic potential', $V_{ion}^{\prime(\alpha)}$, introduced into the uniform electron gas, $\bar{n}$, induces a screening valence electronic density $n_v^{\prime(\alpha)}(r)$. Moreover, the contribution of the corresponding core electrons to the 'auxiliary ionic potential' is influenced by the presence of the valence electrons; consequently $V_{ion}^{\prime(\alpha)}$ and $n_v^{\prime(\alpha)}(r)$ must be evaluated self-consistently. This is performed by using the DFT, solving the Kohn–Sham equations [37], and with the electronic exchange and correlation effects included via the the local density approximation (LDA).

Although $V_{ion}^{\prime(\alpha)}$ is not weak in the core region, it does have the weak-scattering property, since the associated Friedel sum is equal to zero. Then, neglecting all the multiple-scattering contributions, $\Delta n_v(\boldsymbol{r})$ can be approximated by

$$\Delta n_v(\boldsymbol{r}) = n_v(\boldsymbol{r}) - \bar{n} = \sum_i n_v^{\prime(A)}(|\boldsymbol{r} - \boldsymbol{R}_i^{(A)}|) + \sum_j n_v^{\prime(B)}(|\boldsymbol{r} - \boldsymbol{R}_j^{(B)}|) + n_v''(\boldsymbol{r}) \tag{9}$$

where $n_v''(\boldsymbol{r})$ is the valence electronic density induced by $V''(\boldsymbol{r})$. As $V''(\boldsymbol{r})$ is small everywhere, $n_v''(\boldsymbol{r})$ is computed via LRT yielding

$$n_v''(\boldsymbol{r}) = -\bar{n} + \sum_i n_v^{\prime\prime(A)}(|\boldsymbol{r} - \boldsymbol{R}_i^{(A)}|) + \sum_j n_v^{\prime\prime(B)}(|\boldsymbol{r} - \boldsymbol{R}_j^{(B)}|). \tag{10}$$

Here, $n_v^{\prime\prime(A)}(r)$ and $n_v^{\prime\prime(B)}(r)$ are the electron densities that screen, in the linear response, the charge distributions given by $\nu^{(A)}(r)$ and $\nu^{(B)}(r)$ respectively; that is,

$$\tilde{n}_v^{\prime\prime(A)}(q) = -\frac{4\pi}{q^2}\chi(q)\tilde{\nu}^{(A)}(q) \qquad n_v^{\prime\prime(B)}(q) = -\frac{4\pi}{q^2}\chi(q)\tilde{\nu}^{(B)}(q) \tag{11}$$

where the tilde denotes the Fourier transform and $\chi(q)$ is the density response function. In order to maintain consistency with the previous step, the exchange and correlation effects in $\chi(q)$ have been included via a LDA local field. Now, substitution of equation (10) in equation (9) gives

$$n_v(\boldsymbol{r}) = \sum_i n_v^{(A)}(|\boldsymbol{r} - \boldsymbol{R}_i^{(A)}|) + \sum_j n_v^{(B)}(|\boldsymbol{r} - \boldsymbol{R}_j^{(B)}|) \tag{12}$$

which completes the calculation of $n_v(\boldsymbol{r})$.

Now, we turn to the calculation of the local pseudopotentials, $\tilde{v}_{ps}^{(A)}(q)$ and $\tilde{v}_{ps}^{(B)}(q)$, that within LRT reproduce the nonlinear screening charges determined by the NPA method. This is achieved by first 'pseudizing' $n_v^{(A)}(r)$ and $n_v^{(B)}(r)$, in the way described in [38], so as to eliminate the core orthogonality oscillations, leading to the corresponding induced valence electron pseudodensities $n_{ps}^{(A)}(r)$ and $n_{ps}^{(B)}(r)$, from which the corresponding pseudopotentials are obtained via

$$\tilde{n}_{ps}^{(A)}(q) = \chi(q)\tilde{v}_{ps}^{(A)}(q) \qquad \tilde{n}_{ps}^{(B)}(q) = \chi(q)\tilde{v}_{ps}^{(B)}(q). \tag{13}$$

Some comments concerning the assumptions made to obtain the pseudopotentials are now in order. The present approach is based on the physical picture of a simple liquid metallic alloy where the ions are diffusively free and the electronic response to them is treated as a superposition of the single responses to each type of ion. The calculation of the induced valence electronic densities around each type of ion, i.e. $n_v^{(A)}(r)$ and $n_v^{(B)}(r)$, implies that one should solve for each type of ion the Kohn–Sham equations for a system composed of a bare nucleus surrounded by a spherical cavity and embedded in a jellium with a given mean electronic density $\bar{n}$. Moreover, the assumption of spherical symmetry reduces the calculation to solving the radial Kohn–Sham equations.

For the cavity screening functions, $\nu^{(A)}(r)$ and $\nu^{(B)}(r)$, used in the calculation of $n''(r)$, we have chosen a spherical shape. Whereas for a solid system, with a known structure, it would be possible to evaluate explicitly the residual density, $n_r(r)$, for different shapes of the cavity functions, and to choose those which minimize $n_r(r)$, in the case of a liquid system the structure is not known *a priori*. However, in the liquid state what really matters is the ensemble average of the residual density which turns out to be zero, irrespective of the particular shape adopted for the cavity functions, provided that they integrate to the respective ionic valences Z_v^A and Z_v^B respectively. Therefore, we have chosen the simplest approximation—that is, spherical shapes.

The choice of local effective pseudopotentials, as defined through equation (13), is an *ansatz* which avoids the introduction of adjustable parameters while at the same time preserving the full information contained in the calculated NPA-induced valence electronic densities $n_v^A(r)$ and $n_v^B(r)$. In this way, the pseudopotentials are built within the linear response regime, so as to generate the nonlinear screening charges determined by the NPA method. Finally, note that equation (13) uniquely defines the local effective pseudopotentials; this would no longer be the case for nonlocal pseudopotentials.

4. Results

4.1. Calculation of the effective interatomic potentials

As previously indicated, the evaluation of the interatomic pair potentials requires the previous calculation of the induced electronic densities $n_v^A(r)$ and $n_v^B(r)$. Now, each induced density has two parts, $n_v'^{(\alpha)}(r)$ and $n_v''^{(\alpha)}(r)$ ($\alpha = \mathrm{A}, \mathrm{B}$).

For $n_v'^{(\alpha)}(r)$ we have solved the Kohn–Sham equations, in which the exchange and correlation potential has been evaluated within the LDA, using the expression proposed by Vosko *et al* [39] for the exchange and correlation energy density. The technical aspects concerning the solution of the equations are discussed in detail in [40].

For $n_v''^{(\alpha)}(r)$ we have used a density response function, $\chi(q)$, which, in order to maintain consistency with the previous step, incorporates the electronic exchange and correlation effects via a LDA local field factor.

Table 1. Input data for the series Na_xK_{1-x} at $T = 373$ K, studied in this work. ρ is the total ionic number density taken from [41, 42].

$x = x_{Na}$	ρ (Å^{-3})
0.0	0.012 614
0.3	0.014 874
0.4	0.015 805
0.5	0.016 827
0.8	0.020 684
1.0	0.024 217

Now, once the A-type and B-type effective local pseudopotentials, $\tilde{v}_{ps}^{(A)}(q)$ and $\tilde{v}_{ps}^{(B)}(q)$, have been obtained, application of standard second-order perturbation pseudopotential theory leads to the effective interionic pair potentials, $\varphi_{\alpha\beta}(r)$ $(\alpha, \beta = \mathrm{A}, \mathrm{B})$, given by

$$\varphi_{\alpha\beta}(r) = \frac{Z_v^\alpha Z_v^\beta}{r} + \varphi_{ps}^{\alpha\beta}(r) \tag{14}$$

where the Fourier transform of $\varphi_{ps}^{\alpha\beta}(r)$ is given as

$$\tilde{\varphi}_{ps}^{\alpha\beta}(q) = \chi(q)\tilde{v}_{ps}^{\alpha}(q)\tilde{v}_{ps}^{\beta}(q). \tag{15}$$

The present method has been applied to the study of the structural features of the liquid binary alloy Na_xK_{1-x} at $T = 373$ K, and in table 1 we show the specific thermodynamic states for which the present study has been carried out. The total ionic number densities used in the calculations have been taken from the experimental results of van der Lugt and co-workers [41, 42]

First, we show in figure 1 the NPA interatomic pair potentials corresponding to both pure sodium and potassium obtained at a temperature $T = 373$ K. Although several interatomic pair potentials have been proposed for the liquid alkali metals, either based on local or nonlocal pseudopotentials, we have already shown that the NPA-based pair potentials give a good description of the structural [26], thermodynamic [43], and dynamic properties [44, 45, 46] of the liquid alkali metals at thermodynamic conditions near and above melting. Moreover, for liquid Na, we have found [26] that the NPA pair potential is very similar to the 'experimental' one extracted by Reatto *et al* [47] from the measured static structure factor [48].

In figure 1, we have also included the pair potentials obtained by using the simple ECM pseudopotential, $\tilde{v}_{ps}(q) = -4\pi Z_v \cos(qr_c)/q^2$, along with the Ichimaru–Utsumi approximation for the local field factor. The corresponding r_c-values have been chosen so as to match the first peak position of the experimental static structure factor at melting; in this way we have obtained $r_c(\mathrm{Na}) = 0.937$ Å and $r_c(\mathrm{K}) = 1.238$ Å, which are similar to the values usually found in the literature. Comparison between the NPA pair potentials and the ECM ones shows that the two schemes lead to rather similar shapes for the interatomic

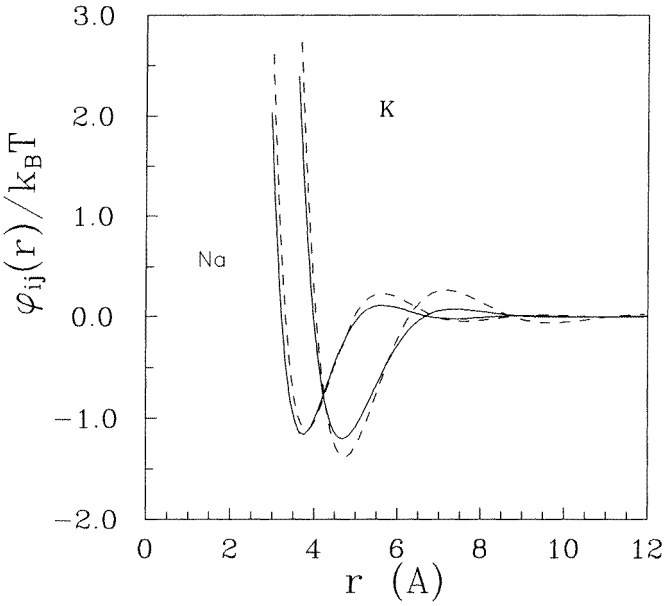

Figure 1. Interatomic pair potentials, $\varphi_{ij}(r)$, for Na and K at $T = 373$ K. The full lines show the NPA results, and the broken lines show the results for the ECM pseudopotential.

pair potentials. In fact, although the repulsive parts are nearly identical, it is observed that some small differences appear: e.g., the Friedel oscillations in the ECM pair potentials are stronger and the principal minimum is a bit deeper in the case of potassium. Rather similar trends were also obtained for the other alkali metals at thermodynamic conditions near melting [26].

Figures 2–4 show the NPA interatomic pair potentials obtained for three different concentrations of the alloy Na_xK_{1-x}; for comparison, we have also included the ECM interatomic pair potentials calculated using the previous r_c-values. First, it is observed that the trends in the changes shown by the $\varphi_{ij}(r)$, as the alloy concentration x_{Na} is varied, are very similar in the NPA and ECM theoretical approaches. In particular, we point out the appreciable changes undergone by $\varphi_{NaNa}(r)$, whereas $\varphi_{KK}(r)$ shows rather small changes as a function of the alloy concentration. In fact, these changes may be explained in terms of the trends suggested by Hafner and Heine [49]; although these trends were obtained within the framework of second-order perturbation theory with the ECM pseudopotential for the bare electron–ion interaction, the conclusions also apply to the NPA-based interatomic pair potentials [25, 26]. According to Hafner and Heine, the trends in the form of the interatomic pair potentials around the nearest-neighbour distance are dominated by the interplay of two parameters (the core radius, r_c, and the mean valence electron density, $\bar{n}$) giving rise to two main effects: the 'core effect' which governs the changes in the repulsive part of the interatomic pair potentials; and the 'amplitude effect' which usually overcomes the other effect, and determines the changes in the amplitude of the Friedel oscillations.

For the $\varphi_{NaNa}(r)$, when the x_{Na} is reduced, the mean electron density in the alloy is decreased, and according to the 'core effect' the repulsive core of the interatomic pair potential is also slightly decreased; this has the effect of uncovering the principal minimum of the interatomic pair potential which becomes deeper and steeper. On the other hand, the

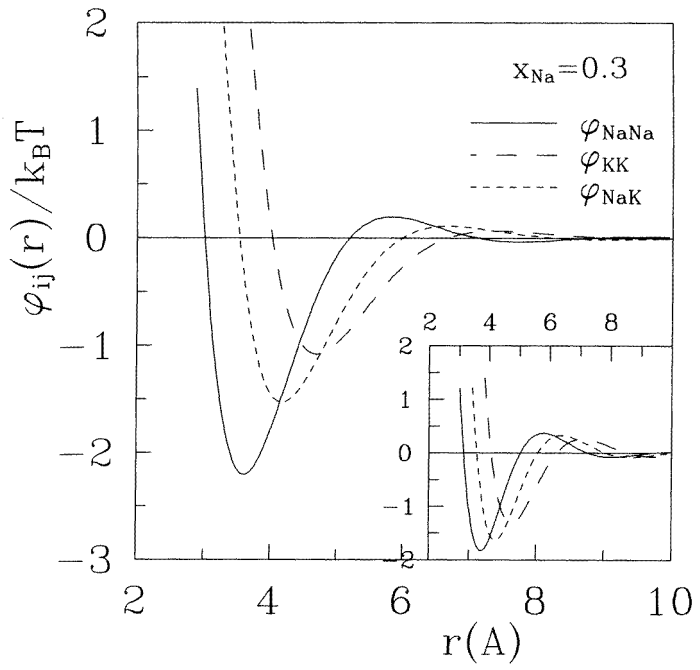

Figure 2. NPA interatomic pair potentials, $\varphi_{ij}(r)$, for the $Na_{0.3}K_{0.7}$ liquid alloy at $T = 373$ K. The inset shows the corresponding results obtained by using the ECM pseudopotentials.

'amplitude effect' produces an increase of the amplitude of the Friedel oscillations and a phase shift towards greater r-values which also gives rise to a further uncovering of the first minimum. Therefore, in the case of the $\varphi_{NaNa}(r)$ the two effects act together, increasing both the depth and width of the principal minimum of the interatomic pair potential, as seen in figures 2–4.

In the case of $\varphi_{KK}(r)$ both effects are rather weak. This is so because now the strength of the 'amplitude effect' is reduced for the range of values of $r_c/\bar{n}$ considered when, starting with pure K, the x_{Na} is increased. In fact, as x_{Na} is increased, the repulsive core slightly grows, and according to the 'amplitude effect', there is also a decrease in the amplitude of the Friedel oscillations and a phase shift towards smaller r-values. Both effects go in the direction of covering the principal minimum of the interatomic pair potential with the net effect of a small decrease in the depth and width of the first minimum.

We point out that although the above trends were obtained within the framework of second-order perturbation theory using the ECM pseudopotential, these trends are also followed by the rather more elaborate NPA pair potentials. However, this does not imply that the use of second-order perturbation theory with the simple ECM pseudopotentials will be an adequate theoretical tool for explaining observed structural properties of the liquid Na_xK_{1-x} alloy. In fact, for all of the x_{Na} considered, appreciable differences are observed between the NPA- and ECM-based interatomic pair potentials; among these we stress that the NPA-based $\varphi_{NaNa}(r)$ is always deeper than the ECM one, whereas the opposite is the case for the $\varphi_{KK}(r)$. As the structural properties are closely linked to the relative magnitudes of the $\varphi_{ij}(r)$ in the alloy, the above-mentioned differences will have far-reaching consequences in the predicted structural properties of the alloy.

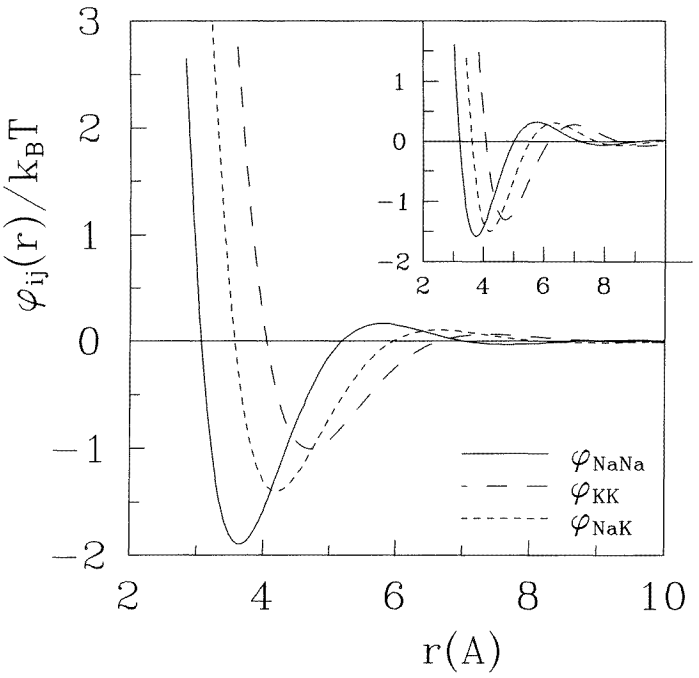

Figure 3. As figure 2, but for the $Na_{0.5}K_{0.5}$ liquid alloy at $T = 373$ K.

4.2. Liquid structure

The calculation of the liquid structure has been carried out by combining the interatomic pair potentials obtained in section 4.1 with the MHNC-REP theory of liquids presented in section 2.

Figure 5 shows the calculated static structure factors for Na and K at $T = 373$ K, along with the corresponding x-ray diffraction data of van der Lugt and co-workers [50, 51] and Waseda [52]. First of all, we must point out the small discrepancies shown by both sets of experimental data concerning the height of the principal peak of the static structure factor, $S(q_{peak})$. In both metals the discrepancy is bigger than 10%. In fact, van der Lugt's data give $S(q_{peak}) \approx 3.1$ for Na and $S(q_{peak}) \approx 2.9$ for K, whereas those of Waseda lead to $S(q_{peak}) \approx 2.7$ and $S(q_{peak}) \approx 2.5$ respectively. In a recent study of the structural properties of the liquid alkali metals, at thermodynamic conditions near melting [26], we have also found a similar discrepancy in the $S(q_{peak})$, with the data of van der Lugt and co-workers always being bigger. In general, there is an overall good agreement between the theoretical $S(q)$ and the experimental data. The positions and amplitudes of the oscillations are well predicted, although the NPA-based results show, for both Na and K, a small shift in the position of the second peak.

Now, figures 6–8 show the partial pair distribution functions, $g_{ij}(r)$, obtained for three concentrations. Following the tendencies pointed out for the $\varphi_{ij}(r)$, it is observed that $g_{NaNa}(r)$ undergoes important changes whereas both $g_{NaK}(r)$ and $g_{KK}(r)$ change slightly. In fact, when the x_{Na} is decreased the height of the main peak of $g_{NaNa}(r)$ increases, as expected from the progressive steepness of the repulsive core of the $\varphi_{NaNa}(r)$, while its position remains practically unchanged. On the other hand, the $g_{NaK}(r)$ remains practically

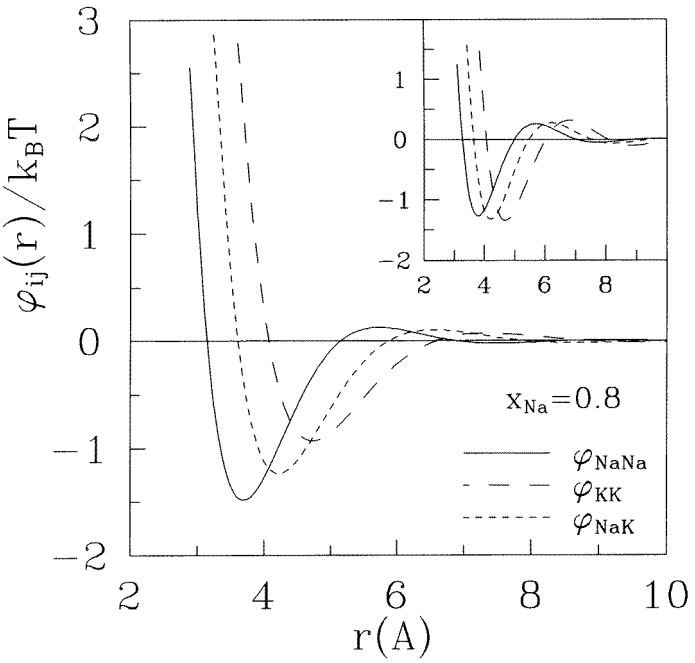

Figure 4. As figure 2, but for the $Na_{0.8}K_{0.2}$ liquid alloy at $T = 373$ K.

constant while the height of the main peak $g_{KK}(r)$ slightly increases and becomes, for $x_{Na} = 0.5$ and 0.3, comparable to that of $g_{NaK}(r)$. For these two concentrations the global configuration suggested by the NPA-based $g_{ij}(r)$ predicts a slight tendency towards phase separation; we will come to this point later.

In figures 6–8 we have also plotted, for comparison, the $g_{ij}(r)$ derived from the ECM interatomic pair potentials. Now, the main peaks of the three $g_{ij}(r)$ have similar heights, with the $g_{NaK}(r)$ becoming the highest for $x_{Na} = 0.5$ and 0.3; now, these features are signalling a very weak tendency towards heterocoordination.

As already pointed out, van der Lugt and co-workers (see [13]) have performed both x-ray and neutron diffraction experiments for the Na_xK_{1-x} liquid alloy at several concentrations and temperatures. Figure 9 shows, as a function of the concentration, two main experimental structural features of this alloy, namely the position, q_{peak}, and height of the first peak of the total x-ray measured structure factor, $S(q_{peak})$; they are compared with the theoretical results of this paper, where the theoretical x-ray total structure factor has been computed by using the atomic form factors given in [53]. In figure 9 we have also included the experimental results for q_{peak} obtained by Orton *et al* [54], which are always slightly bigger than those of van der Lugt *et al* (see [13]). It is observed that the present theoretical results are always bracketed by the two sets of experimental results; this gives further confidence in the accuracy of the present theoretical results which, on the other hand, are similar to those obtained for the pure metals. For $S(q_{peak})$, it is now observed that the experimental results are bracketed by the two sets of theoretical results which closely follow, as the concentration changes, the trends shown by the experimental results. However, now the theory/experiment discrepancy is around 10%, with the NPA-based and ECM-based results underestimating and overestimating, respectively, the experimental data.

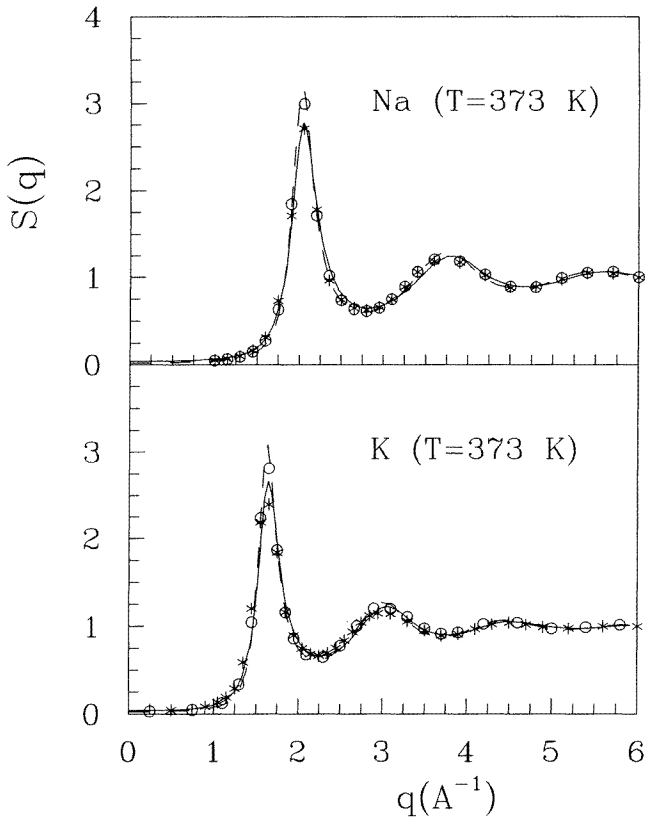

Figure 5. Static structure factors for Na and K at $T = 373$ K obtained using the MHNC-REP approximation. The full lines show the results for the NPA interatomic pair potentials, whereas the broken lines show the results for the ECM pseudopotential. The asterisks represent the x-ray data of Waseda [52] and the open circles show the x-ray data of van der Lugt and co-workers [50, 51].

Nevertheless, the discrepancy must be treated with some caution. As we already pointed out, in the case of the pure metals the discrepancy between van der Lugt's data (see [50]) for $S(q_{peak})$ and Waseda's [52] data is also around 10%, with the latter data being much closer to the NPA-based results. In any case, it seems reasonable to conclude that the NPA-based results are more accurate than the ECM-based ones, as the former results are between the two sets of experimental results.

Figures 10–12 show a comparison, for three concentrations, between the experimental x-ray total structure factors and the theoretical ones. In general, an overall good agreement between theory and experiment is obtained for all of the concentrations, with the NPA-based results showing a small phase shift in the region between the first minimum and the second maximum of the total structure factor, but being more accurate than the ECM-based results for the region $q \leqslant q_{peak}$.

Now, we return to the study of the possible existence of deviations from an ideal behaviour in the Na_xK_{1-x} liquid alloy. For this purpose, the Bhatia–Thornton (BT) [55] partial structure factors are ideally suited. In a binary system, three BT partial structure factors are defined: the concentration–concentration ($S_{CC}(q)$), the number–number

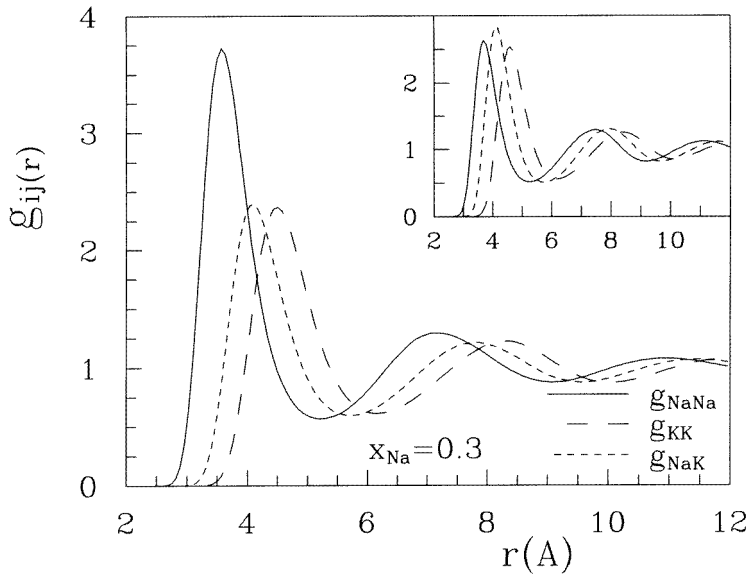

Figure 6. Partial pair distribution functions, $g_{ij}(r)$, for the $Na_{0.3}K_{0.7}$ liquid alloy at $T = 373$ K. The inset shows the corresponding results obtained by using the ECM pseudopotentials.

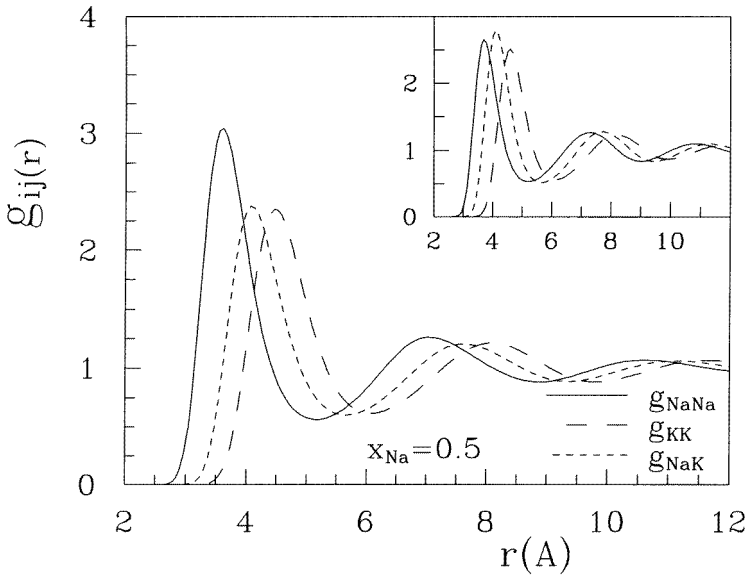

Figure 7. As figure 6, but for the $Na_{0.5}K_{0.5}$ liquid alloy at $T = 373$ K.

($S_{NN}(q)$), and the number–concentration ($S_{NC}(q)$) partial structure factors; they are readily computed from the partial pair distribution functions, $g_{ij}(r)$, previously obtained with the MHNC-REP approximation introduced in section 2. Moreover, the BT partial structure factors have the advantage that their long-wavelength limit, which has proved to be very

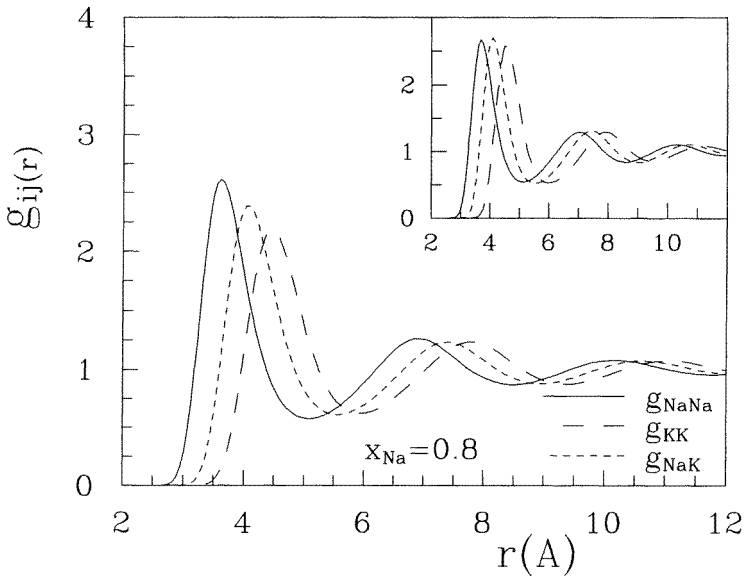

Figure 8. As figure 6, but for the $Na_{0.8}K_{0.2}$ liquid alloy at $T = 373$ K.

useful in obtaining microscopic information in a liquid alloy, can also be derived from thermodynamic magnitudes; this is very helpful because of the practical difficulties of measuring, via diffraction experiments, the partial structure factors at low q-values. Now, the long-wavelength limit of the BT partial structure factors can be obtained from

$$S_{CC}(0) = NK_BT\left(\frac{\partial^2 G}{\partial x_1^2}\right)^{-1}_{N,P,T} = (1-x_1)\left(\frac{\partial \ln a_1}{\partial x_1}\right)^{-1}_{N,P,T} \tag{16}$$

$$S_{NN}(0) = \rho K_BT\kappa_T + \delta^2 S_{CC}(0) \tag{17}$$

$$S_{NC}(0) = -\delta S_{CC}(0) \tag{18}$$

where N is the total number of particles, G is the Gibbs free energy, a_i and x_i are the thermodynamic activity and concentration of component i respectively, κ_T is the isothermal compressibility, and δ is a dilatation factor given by

$$\delta = \frac{v_1 - v_2}{x_1 v_1 + (1-x_1)v_2} \tag{19}$$

where v_i is the partial volume per atom of component i.

Figure 13 shows, as a function of the concentration, the theoretical results for $S_{CC}(0)$ obtained from both the NPA-based and ECM-based interatomic pair potentials. In the figure we have included the experimental data derived by van der Lugt and co-workers (see [13]) from their small-angle x-ray scattering experimental results, and also the results derived, according to equation (16), from the activity measurements of Cafasso *et al* [11] and Hultgren *et al* [12]. The three sets of experimental data, which show some small discrepancies among themselves, do clearly indicate that the ions in the Na_xK_{1-x} liquid alloy have a slight preference for self-coordination; in other words, there is a very mild phase-separating tendency. In fact, this is the behaviour predicted by the present NPA-based theoretical results which closely follow Hultgren's data. On the other hand, the

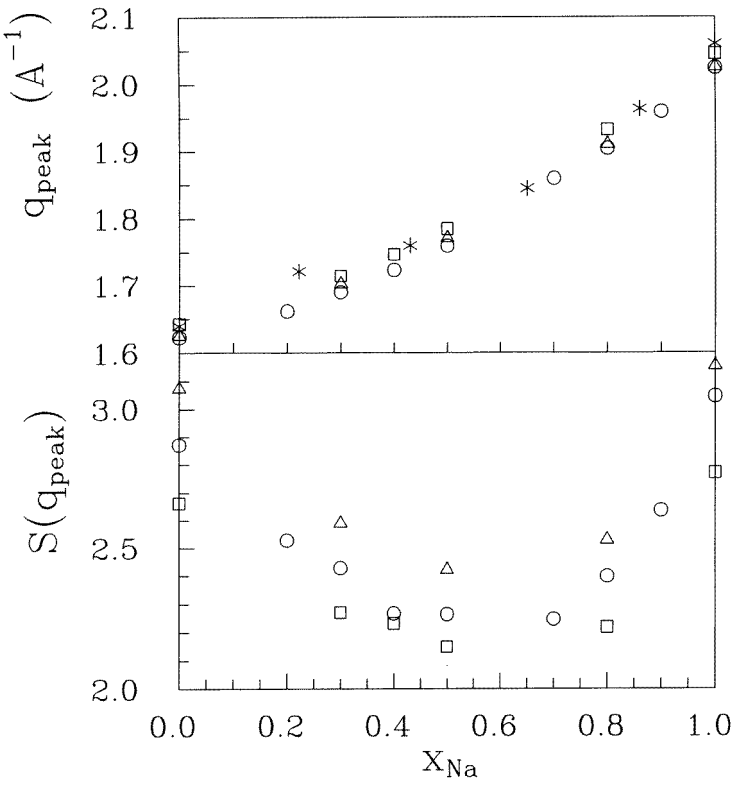

Figure 9. Top panel: the position of the first peak of the total x-ray structure factor. Bottom panel: the height of the first peak of the total x-ray structure factor. Squares: NPA-based results. Triangles: ECM-based results. Open circles: experimental results [13]. Asterisks: experimental results [54].

ECM-based theoretical results predict a nearly ideal behaviour with a very weak tendency towards heterocoordination.

Figure 14 shows a further comparison for $S_{NN}(0)$ and $S_{NC}(0)$, where the corresponding experimental data have been derived from the activity measurements of Hultgren *et al* [12], the experimental molar volumes of the system of van der Lugt *et al* [41], the sound velocity data of Kim *et al* [56], and the specific heat data of Lyon [57]. Once again, the degree of accuracy of the NPA-based results is very good, and similar to that obtained for $S_{CC}(0)$.

Finally, we stress that the accurate structural results presented in this paper are basically due to the NPA-based interatomic pair potentials. We have calculated the liquid structural functions of this alloy, by using the variational hypernetted-chain-approximation theory of liquids [31], and the results obtained are nearly identical to those presented in this work.

5. Conclusions

We have extended the NPA model to the case of simple metallic alloys and we have applied it to the study of the structural and ordering properties of the of the Na_xK_{1-x} liquid alloy at $T = 373$ K. The combination of the NPA method to obtain the interatomic pair potentials

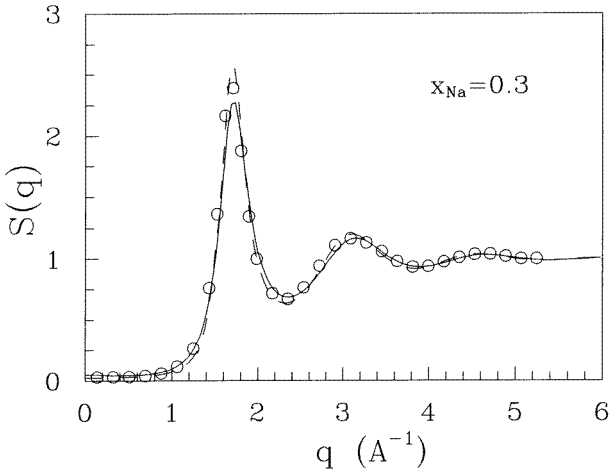

Figure 10. The total x-ray static structure factor, $S(q)$, for the $Na_{0.3}K_{0.7}$ liquid alloy at $T = 373$ K. Full line: NPA-based results. Broken line: ECM-based results. Open circles: experimental results [13].

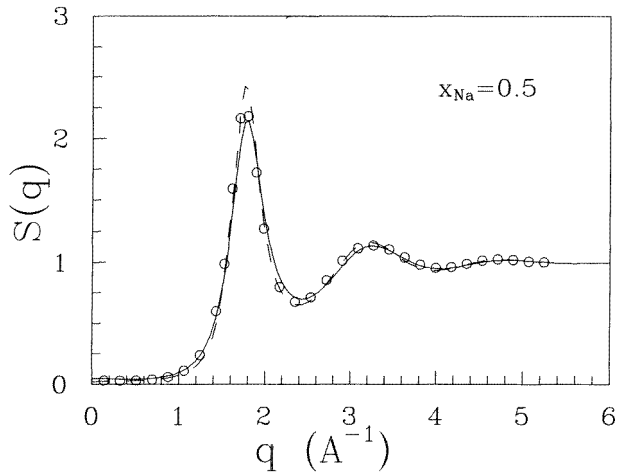

Figure 11. The total x-ray static structure factor, $S(q)$, for the $Na_{0.5}K_{0.5}$ liquid alloy at $T = 373$ K. The key is the same as in figure 10.

with the MHNC-REP theory of liquids to obtain the liquid static structure gives rise to a theory which is wholly free of adjustable parameters, using the atomic numbers and the thermodynamic state under study as the only input data. The present NPA formulation for a simple liquid-metallic alloy, A_xB_{1-x}, starts from the screening charges around the A-type and B-type bare ions embedded into an homogeneous electron gas, which yields A-type and B-type effective local pseudopotentials, and finally the interatomic pair potentials in the alloy. The interatomic pair potentials obtained show, as functions of the mean electronic density in the alloy, similar trends to those obtained by using the simple ECM pseudopotentials. These results confirm and extend the general analysis of Hafner and Heine

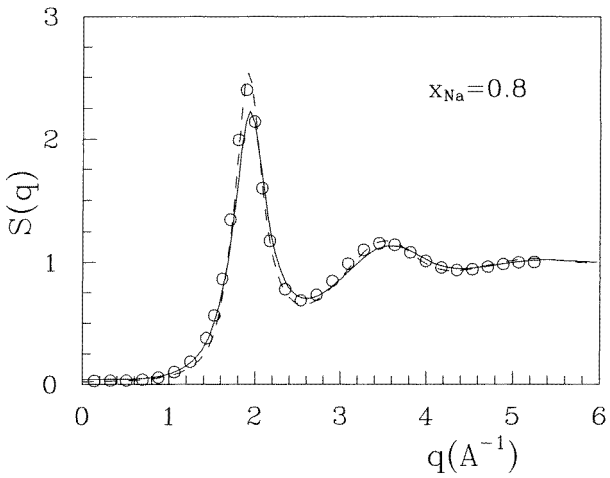

Figure 12. The total x-ray static structure factor, $S(q)$, for the $Na_{0.8}K_{0.2}$ liquid alloy at $T = 373$ K. The key is the same as in figure 10.

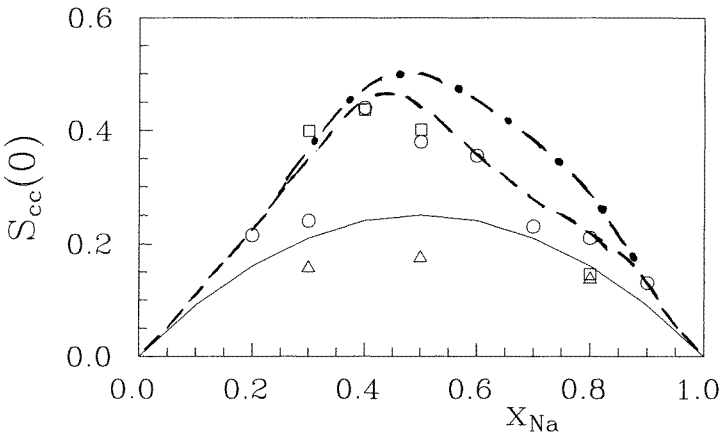

Figure 13. The concentration dependence of $S_{CC}(0)$ for the Na_xK_{1-x} liquid alloy at $T = 373$ K. Squares: NPA-based results. Triangles: ECM-based results. Continuous line: ideal solution result, $S_{cc}(0) = x(1 - x)$. Open circles: experimental results from van der Lugt *et al* [13]. Dash-dotted line: experimental results from the activity measurements of Cafasso *et al* [11]. Chain line: experimental results from the activity measurements of Hultgren *et al* [12].

[49] about the variations of the interatomic pair interactions and the relationship to both solid and liquid structures.

The results obtained for the liquid structural properties of the Na_xK_{1-x} liquid alloy at $T = 373$ K show a good agreement with the experiment, which we consider very rewarding given that our calculations are completely free of adjustable parameters. In fact, as far as we are aware these are the first parameter-free theoretical calculations which predict a weak phase-separating tendency for this alloy. On the other hand, our study shows that although the ECM-based interatomic pair potentials are able to account for the observed total x-ray structure factor, they fail to predict the ordering properties of the alloy.

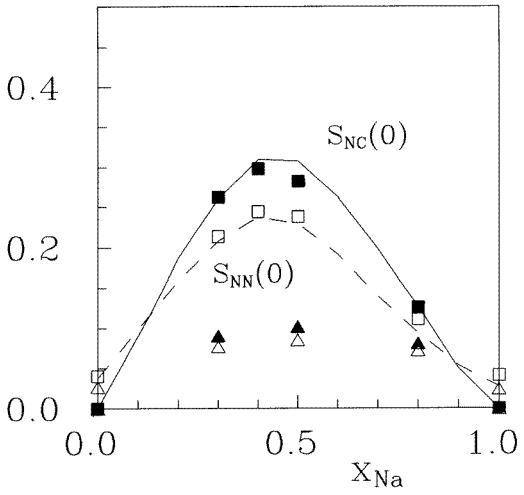

Figure 14. The concentration dependence of $S_{NC}(0)$ and $S_{NN}(0)$ for the Na_xK_{1-x} liquid alloy at $T = 373$ K. Filled and open squares: NPA-based results for $S_{NC}(0)$ and $S_{NN}(0)$ respectively. Filled and open triangles: ECM-based results for $S_{NC}(0)$ and $S_{NN}(0)$ respectively. Continuous and broken lines: experimental results for $S_{NC}(0)$ and $S_{NN}(0)$ respectively.

Finally, we point out that the present NPA + MHNC-REP theoretical approach lacks self-consistency because the screening charges around the A-type and B-type ions should be computed, not for each ion immersed into an homogeneous electron gas, but taking into account both the structure of the alloy and the presence of two different kinds of ion. Therefore, the present NPA approach must be considered as a first step in a whole self-consistent procedure where the partial pair distribution functions, $g_{ij}(r)$, obtained should be introduced into the NPA method to again compute the screening charges, and so forth. We are currently working on this procedure, and the results will be reported in due course.

Acknowledgments

This work was supported by the DGICYT of Spain through grant number PB92-0652-CO3. We gratefully acknowledge Professor van der Lugt for sending detailed information on the experimental results for the Na_xK_{1-x} liquid alloy.

References

[1] Young W H 1992 *Rep. Prog. Phys.* **55** 1769
[2] Balucani U and Zoppi M 1994 *Dynamics of the Liquid State* (Oxford: Oxford University Press)
[3] Singh R N 1987 *Can. J. Phys.* **65** 309
[4] Enderby J E and North D M 1968 *Phys. Chem. Liq.* **1** 1
[5] Henninger E H, Buschert R C and Heaton L 1966 *J. Chem. Phys* **44** 1758
[6] Abowitz G and Gordon R B 1962 *J. Chem. Phys* **37** 125
[7] van der Lugt W, Devlin J F, Hennephof J and Leenstra R M 1973 *The Properties of Liquid Metals* ed S Takeuchi (London: Taylor and Francis) p 345
[8] Amaral J E and Letcher S V 1974 *J. Chem. Phys.* **61** 92
[9] Flinn J M, Gupta P K and Litovitz T A 1974 *J. Chem. Phys.* **60** 4390
[10] Kim M G and Letcher S V 1971 *J. Chem. Phys.* **55** 1164

[11] Cafasso F A, Khanna V M and Feder H M 1967 *Adv. Phys.* **16** 535
[12] Hultgren R R, Orr R L, Anderson P D and Kelly K K 1963 *Selected Values of Thermodynamic Properties of Metals and Alloys* (New York: Wiley)
[13] Alblas B P and van der Lugt W 1980 *J. Phys. F: Met. Phys.* **10** 531
Alblas B P, van der Lugt W, van der Valk H J L, de Hosson J T M and van Dijk C 1980 *Physica* B **101** 177
[14] Bhatia A B and March N H 1972 *Phys. Lett.* **41A** 397
[15] Alonso J A and March N H 1982 *Physica* B **114** 67
[16] Umar I H, Meyer A, Watabe M and Young W H 1974 *J. Phys. F: Met. Phys.* **4** 1691
[17] Hafner J 1977 *Phys. Rev.* A **16** 351
[18] Singh R N 1981 *J. Phys. F: Met. Phys.* **11** 389
[19] Mori H, Hoshino K and Watabe M 1991 *J. Phys.: Condens. Matter* **3** 9791
[20] Ashcroft N W 1966 *Phys. Lett.* **23** 48
[21] Hasegawa M, Hoshino K, Watabe M and Young W H 1990 *J. Non-Cryst. Solids* **117/118** 300
[22] Dagens L 1973 *J. Physique* **34** 879; 1975 *J. Physique* **36** 521
[23] Perrot F 1990 *Phys. Rev.* A **42** 4871
[24] Perrot F and March N H 1990 *Phys. Rev.* A **41** 4521; 1990 *Phys. Rev* A **42** 4884
[25] González L E, Meyer A, Iniguez M P, González D J and Silbert M 1993 *Phys. Rev.* E **47** 4120
[26] González L E, Gonzalez D J and Hoshino K 1993 *J. Phys.: Condens. Matter* **5** 9261
[27] Rosenfeld Y and Ashcroft N W 1979 *Phys. Rev.* A **20** 1208
[28] Percus J K and Yevick G J 1958 *Phys. Rev.* **110** 1
[29] Verlet L and Weiss J J 1972 *Phys. Rev.* A **5** 939
Henderson D and Grundke E W 1975 *J. Chem. Phys.* **63** 601
[30] Labik S and Malijevsky A 1989 *Mol. Phys.* **67** 431
[31] González L E, González D J and Silbert M 1992 *Phys. Rev.* A **45** 3803
[32] Lado F, Foiles S M and Ashcroft N W 1983 *Phys. Rev.* A **28** 2374
[33] González L E, González D J and Silbert M 1991 *Physica* B **168** 39
[34] Levesque D, Weis J J and Chabrier G 1991 *J. Chem. Phys.* **94** 3096
[35] Mori H, Hoshino K and Watabe M 1992 *J. Phys. Soc. Japan* **61** 1218
[36] Mori H, Hoshino K and Watabe M 1993 *J. Non-Cryst. Solids* **156/158** 85
[37] Kohn W and Sham L J 1965 *Phys. Rev.* **140** 1133
[38] Manninen M, Jena P, Nieminen R M and Lee J K 1981 *Phys. Rev.* B **24** 7057
[39] Vosko S H, Wilk L and Nussair M 1980 *Can. J. Phys.* **58** 1200
[40] González L E 1992 *PhD Thesis* Universidad de Valladolid
[41] Huijben M J, van Hasselt J P, van der Weg K and van der Lugt W 1976 *Scr. Metall.* **10** 571
[42] Potter P E, Kagan D N, Le Claire A D and van der Lugt W 1985 *Handbook of Thermodynamic and Transport Properties of Alkali Metals* ed R W Ohse (Oxford: Blackwell Scientific) ch 9.4
[43] González L E, González D J, Silbert M and Alonso J A 1993 *J. Phys.: Condens. Matter* **5** 4283
[44] Canales M, Padró J A, González L E and Giró A 1993 *J. Phys.: Condens. Matter* **5** 3095
[45] Canales M, González L E and Padró J A 1994 *Phys. Rev.* E **50** 3656
[46] González L E, Gonzalez D J and Canales M 1996 *Z. Phys.* at press
[47] Reatto L, Levesque D and Weis J J 1986 *Phys. Rev.* A **33** 3451
[48] Greenfield A J, Wellendorf J and Wiser N 1971 *Phys. Rev.* A **4** 1607
[49] Hafner J and Heine V 1983 *J. Phys. F: Met. Phys.* **13** 2479
[50] Huijben M J and van der Lugt W 1979 *Acta Crystallogr.* A **35** 431
[51] van der Lugt W and Alblas B P 1985 *Handbook of Thermodynamic and Transport Properties of Alkali Metals* ed R W Ohse (Oxford: Blackwell Scientific) ch 5.1
[52] Waseda Y 1980 *The Structure of Non-Crystalline Materials* (New York: McGraw-Hill)
[53] 1969 *International Tables for X-Ray Crystallography* vol 4 (Birmingham: Kynoch) p 41
[54] Orton B R, Shaw B A and Williams G I 1960 *Acta Metall.* **8** 177
[55] Bhatia A B and Thornton D E 1970 *Phys. Rev.* B **2** 3004
[56] Kim M G, Kamp K A and Letcher S V 1970 *Department of Physics, University of Rhode Island, Kingston, Final Report* RI02881
[57] Lyon R N 1952 *Liquid Metal Handbook: NaK Supplement* (Washington, DC: US Government Printing Office)